

Integrated acoustic and acousto-optic filters using domain inversion

D. Yudistira, D. Janner

ICFO-Institut de Ciències Fotoniques
Castelldefels (Barcelona), Spain
dedit.yudistira@icfo.es

V. Pruneri

ICFO-Institut de Ciències Fotoniques
Castelldefels (Barcelona), Spain
ICREA -Institució Catalana de Recerca i Estudis Avançats
Barcelona, Spain

Abstract—Domain inversion superlattices combined with co-planar electrodes allow novel waveguide acoustic and acousto-optic filtering. In this paper we show that efficient devices can be achieved through an appropriate fabrication of domain inverted and electrode geometries.

Domain inversion; acoustic superlattices; acousto-optics filters.

I. INTRODUCTION

In the last decades, the introduction of interdigitated transducers (IDTs) [1] to generate surface acoustic wave (SAW) in ferroelectric crystals, lead to the spreading of acoustic-based devices in many fields. Among the applications are: RF filter for wireless communications, non-destructive testing (NDT), and bio-medical sensing. Recently, the use of periodically poled lithium niobate (PPLN) in combination with coplanar RF electrodes was used for SAW and bulk waves in novel configurations, named acoustic superlattices (ASLs) [2]. One of the main advantages of ASL based transducers is that the elastic wavelength is related to the period Λ of the PPLN compared to IDTs' period that needs to be $\Lambda/2$. Moreover, the coplanar electrode configuration is much simpler and easier to impedance-match.

The combination of acoustic and optical signals brings many interesting applications, particularly in the field of polarization converters. Acousto-optic (AO) polarization converters are key elements in many photonic applications, such as wavelength division multiplexing (WDM), spectral filtering of supercontinuum sources. State-of-the-art integrated AO filters typically combine IDTs and optical medium (waveguide) in a single piezoelectric crystal. The potential drawback of using IDTs for this device, however, lies in the fact that the optical waveguide is usually covered by the metallic layer of the IDTs, thus increasing the optical loss. Employing ASL for acoustic wave generation can potentially overcome the loss issue [3].

In this work we will present recent results and improved geometries for acoustic wave generation based on ASL using co-planar linear electrodes and on their application in AO filters. Along the way we demonstrate the generation of

acoustic longitudinal bulk wave (L-BAW) with high efficiency using a tapered electrode on ASL.

II. SUPERLATTICE COUSTIC FILTERS

Co-planar electrode geometry is employed allowing the electric field to be confined in the crystal region between the electrodes and close to the substrate surface[4]. This allows for direct excitation of both SAW and bulk acoustic waves, reported for the first time in ref. 2.

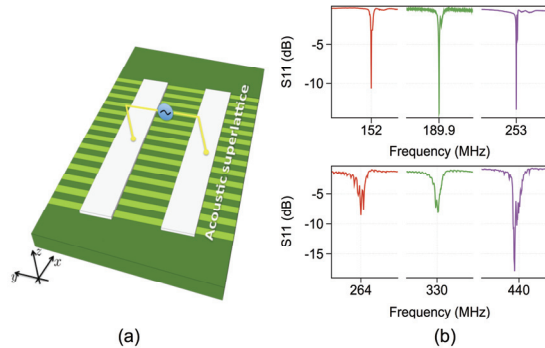


Figure 1. (a) Proposed coplanar electrode ASL transducer. (b) S_{11} for SAW (upper) and L-BAW (lower) generation in different ASL's period Λ .

The scheme of the fabricated device is outlined in Fig. 1(a). The ASLs were prepared on a 500 μm thick ZX-cut LiNbO₃ substrate with various lattice periods $\Lambda=15, 20, \text{ and } 25 \mu\text{m}$ with total length 10 mm. The domain inversion was realized through electric field poling and 200 nm-thick coplanar aluminum (Al) electrodes oriented along the x-axis were deposited on the ASL. The electrode width was chosen to be 100 μm with a metallization ratio (MR) of 0.5. The RF characterization shown in Fig. 1(b) was performed with PNA-X Agilent network analyzer. In the upper part of Fig. 1(b) the measured dips in the S_{11} correspond to the resonance frequencies $f_{\text{SAW}}= 253, 189.7, \text{ and } 152 \text{ MHz}$. At those frequencies the SAW velocities are 3795, 3794, and 3800 m/s, respectively. The comparison with the theoretical velocity of SAW on ZX-cut LiNbO₃ is 3798 m/s, confirming SAW generation. As reported in Fig. 1(b)-bottom, L-BAW that travels with $v_{\text{L-BAW}}=6600 \text{ m/s}$ was also observed with resonance frequencies measured at around 440, 330, and 264

MHz. There is thus a good agreement between calculated and measured frequencies for both SAW and L-BAW. Furthermore, the transduction efficiency of the SAW represented by the effective electromechanical coupling coefficient is about 0.3 %, which is close to 0.53 % obtained from the calculation for ZX-cut LiNbO₃.

III. SUPERLATTICE ACOUSTO-OPTIC FILTERS

The above ASL transducer configuration was used for AO filters. As the ASL transducer is able to generate both SAW and L-SAW, two types of AO device were considered depending on the type of the acoustic wave being employed, namely surface AO and bulk AO filters. In both cases, the AO filtering relies on the transverse electric (TE) to transverse magnetic (TM), or vice versa (TM to TE), polarization conversion of optical wave. The conversion efficiency between TE-TM is defined by $\eta(\Delta=0)=P_M(x=L_i)/P_E(x=0)=\sin^2(\kappa L_i)$, where κ denotes the coupling coefficient and L_i is the interaction length.

For surface AO filter, a mono-modal Ti-LiNbO₃ optical waveguide was fabricated. The waveguide was positioned parallel to and at the center between the electrodes. The edges of ASL were polished at $\theta=8^\circ$ to minimize back reflection from the acoustic wave.

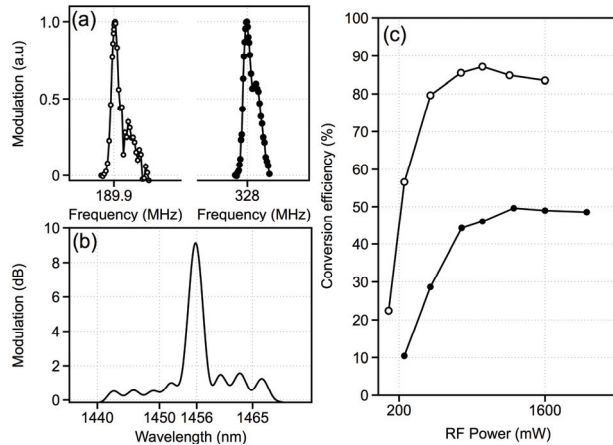


Figure 2. (a) AO modulation of (left) bulk and surface (right) AO filter as a function of RF frequency for RF power of 500 mW. (b) AO modulation vs optical wavelength from surface AO filter. (c) Power conversion efficiency versus RF power from (opened circle) surface AO and (filled circle) bulk AO, respectively.

A Supercontinuum laser source was used to generate a broad spectrum in the wavelength region of interest. To couple the light into and out of the device, a pair of fiber collimator and of single mode fiber block was used for the bulk AO and surface AO samples, respectively. For acoustic wave generation, an amplified RF signal generator was employed and finally an Optical Spectrum Analyzer (OSA) was used to monitor the optical output.

Measurements were carried out using various RF input power P_{RF} ranging from 200 mW to 1600 mW. For each P_{RF} , RF frequency (f_{RF}) was swept around resonance frequency of the ASL transducer with $\Lambda = 20 \mu\text{m}$, $f_{SAW}(f_{BAW})$, $f_{SAW}=189.7$

MHz and $f_{BAW}=330$ MHz (Fig. 2(a)). After that, the optical output was measured around the phase matching wavelengths, $\lambda_S=1456$ nm (surface AO) and $\lambda_B=1472$ nm (bulk AO), respectively. The result of surface AO filter is shown in Fig. 2(b); the -3-dB optical bandwidth was measured around $\Delta\lambda_S=2.51$ nm. The polarization conversion efficiency (η), i.e. the ratio between converted and transmitted power in the absence of RF signal, as a function of RF power for surface and bulk AO is shown in Fig. 2(c).

IV. TAPERED ELECTRODES ON ASL

With straight co-planar electrodes, the surface AO device shows good performance while the bulk AO device does not perform as good as the surface one (Fig. 2(c)). For this reason a special design based on a coplanar curved electrode approach is proposed to increase the efficiency of the bulk AO device. Using a tapered geometry for the RF electrodes, an improved impedance matching at the frequencies of bulk waveguides can be obtained [5].

The MR was fixed at 0.5 along x-axis and the ASL transducer with period Λ of 15 μm was used. Fig. 3 shows a broader S11 spectrum as a result of tapered electrode. A strong dip (-60 dB) at frequency around 440 MHz was obtained showing a quite large transduction from microwave to acoustic wave (L-BAW) compared to the ASL using uniform (straight) electrode shown previously. These results are expected to improve the bulk AO. AO measurements are being performed and will be presented at the conference.

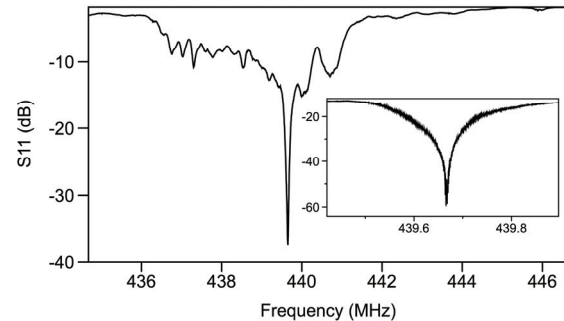


Figure 3. S11 as a function of RF frequency for L-BAW from ASL transducer with curved electrode. Inset is an expanded view around the dip.

REFERENCES

- [1] R. M. White and F. W. Voltmer, "Direct piezoelectric coupling to surface elastic waves", App. Phys. Lett., vol.7, pp. 314-316, 1965.
- [2] D. Yudistira, S. Benchabane, D. Janner and V. Pruneri, "Surface acoustic wave generation in zx-cut linbo₃ superlattices using coplanar electrodes", App. Phys. Lett., vol.95, no.5, pp. 052901, 2009.
- [3] D. Yudistira, D. Janner, S. Benchabane and V. Pruneri, "Integrated acousto-optic polarization converter in a ZX-cut LiNbO₃ waveguide superlattice", Opt. Lett., vol.34, no.20, pp. 3205-3207, 2009.
- [4] Y.-q. Lu, Y.-y. Zhu, Y.-f. Chen, S.-n. Zhu, N.-b. Ming and Y.-J. Feng, "Optical properties of an ionic-type phononic crystal", Science, vol.284, no.5421, pp. 1822-1824, 1999.
- [5] N. Goto and Y. Miyazaki, "Design of tapered SAW waveguide for wavelength-selective optical switches using weighted acoustooptic interaction", Electrical Engineering in Japan, vol.154, no.1, pp. 36-46 2006.